Available online at www.sciencedirect.com
SCIENCE DIRECT®
Optics Communications 245 (2005) 113–124
OPTICS COMMUNICATIONS
www.elsevier.com/locate/optcom

Phase joint transform sequential correlator for nonlinear binary correlations

Joaquín Otón [a], Pascuala Garcia-Martinez [a], Ignacio Moreno [b], Javier Garcia [a,*]

[a] Departament d'Optica, Facultat de Fisica, Universitat de València. c/Dr. Moliner, 50. E-46100, Burjassot, València, Spain
[b] Departamento de Ciencia y Tecnología de Materiales, Universidad Miguel Hernández Avda, Ferrocarril s/n, E-03202 Elche (Alicante), Spain

Received 27 July 2004; received in revised form 15 October 2004; accepted 18 October 2004

Abstract

We study the performance of nonlinear optical correlations using a joint transform correlator that operates in phase-only spatial light modulation at input joint transform plane. Amplitude input nonlinear optical time sequential correlations have shown better discrimination and noise robustness than conventional linear correlations. Those nonlinear correlations are based on decomposing the reference and the target into binary slices and to add the contribution of all linear correlations between them. Those correlations can be easily implemented using a conventional joint transform correlator. However, the system has poor efficiency and low cross-correlation peak intensity, mainly because of the spatial light modulators working in amplitude mode. We use a phase-transformed input joint transform correlator in order to increase the efficiency and the discrimination. The phase morphological correlation and the phase sliced orthogonal nonlinear generalized correlation are implemented optically. We applied the method to images degraded with high degrees of substitutive noise and nonoverlapping background noise. Results show that those nonlinear phase input-encoded correlations detect the target with high discrimination capability in cases where other well-known methods fall.

PACS: 42.79.H; 42.30; 42.30.S
Keywords: Pattern recognition; Nonlinear correlations; Joint transform correlator; Phase codification

1. Introduction

The joint transform correlator (JTC) has been known for many time as a convenient way of optically correlating two input images [1,2]. Most JTCs use an amplitude spatial light modulator

* Corresponding author. Tel.: +34963544611; fax: +34963544715.
E-mail address: javier.garcia.monreal@uv.es (J. Garcia).

0030-4018/$ - see front matter © 2004 Elsevier B.V. All rights reserved.
doi:10.1016/j.optcom.2004.10.044

(SLM) to input the joint transform data into the optical Fourier transform system that produces the output peaks [3]. The introduction of some nonlinearities such as thresholding the joint power spectrum in the JTC has shown to improve substantially the discrimination [4,5]. However, in such cases the input is introduced in the JTC as intensity distribution. Because of that, the system has poor efficiency and low cross-correlation peak intensity, mainly because of the fundamentally poor diffraction efficiency and high absorption intrinsic to gratings written on amplitude modulators. In attempt to overcome this problem, many researchers have used a phase SLM instead. The optical efficiency of a system using a phase SLM is usually high because the SLM has no absorption. So, the influence of the codification of the amplitude distributions as phase functions in optical correlation has been widely investigated, both in the Fourier plane (codification of the filter) [6–9] and in the input image [10–12]. Those works refer mainly to Vander Lugt correlators. However, the application to joint transform correlator is quite direct. In fact previous to those phase input codification systems, Johnson et al. [13] analyzed the performance of a JTC in which the joint transform intensity distribution is converted onto a phase distribution before being input to the second Fourier transform system. Like Vander Lugt phase only filters, the system proposed by Johnson et al. [13] improves the light efficiency and so the discrimination capability, however with multiple test objects they show that multiple output peaks appears due to nonlinearities in the system, and some of those peaks might be false alarms. The same result was obtained for the case of binarization nonlinearities in the JTC Fourier plane [14]. Nevertheless in all previous works the conversion from amplitude distribution to phase was done in the Fourier plane. Lu et al. [15] introduced the concept to using phase-encoded input representation in a joint transform correlator. In this system, a phase-only joint input is used, the joint power spectrum is recorded and then sent back on the liquid crystal television (LCTV) panel which is modulated in amplitude mode for the correlation operation. The authors justified mathematically the pattern discrimination improvements in comparison with amplitude conventional joint transform correlators. Afterwards Lu and Yu [16] showed a detailed analysis on the performance of system proposed in [15]. They studied the advantages in pattern discriminability, detection efficiency and noise robustness compared to conventional JTC. An analogous study was done also by Erbach et al. [17]. The difference was that for Ref. [17] the JPS was encoded as a phase distribution. Furthermore Ledesma et al. [18] proposed different methods for pattern recognition that used phase mode in joint transform correlator. They considered three different codifications of the JPS, one in phase encoding of the JPS, the second the binarization of the JTC and the third one was extracting the phase of the joint transform correlator. They confirmed the improvements of those systems in comparison with amplitude JTC. In a more recent paper, Iemmi and La Mela [19] defined a JTC were the joint input scene is introduced in phase modulation and the JPS is recorded dynamically in amplitude using a photorefractive material. However, a preprocessed reference that provides the phase-only information of the target in the Fourier plane is used to improve the pattern discriminability. Regarding with noise robustness, Pagé and Goudail [20] showed that if the object to be located is perturbed with nonoverlapping background noise, phase encoding can improved the performance compared with amplitude encoding. Other papers discuss the phase encoding in JTC introducing a phase mask in the input plane in order to reduce the influence of the extraneous signals, namely autocorrelations or complex conjugate correlations [21,22]. Note that phase encoding methods improve the discrimination ability of the process, and as a consequence they are more sensitive to changes in the objects, namely illumination, shadowing or geometrical distortions.

All methods mentioned above deal with different ways to obtain improvements in light efficiency and pattern discriminability using phase spatial light modulators, however all of them use a linear correlation idea. From the last six years we have proposed nonlinear correlations characterized by a better discrimination for pattern recognition than linear filters such as conventional matched fil-

ters and even other well-known filtering techniques like inverse filtering [23–25]. These correlations use the addition of many linear correlations between the elements of a binary decomposition of the input scene and of the reference object. They can be implemented optically using a time sequential joint transform correlator (JTC) for adding the joint power spectra of all the binary slices [26,27]. In this paper, we use the phase-transformed input joint transform correlation in the optical implementation of the nonlinear correlation. We compared the correlation obtained with previous methods and the nonlinear correlations. Better discrimination and high noise robustness are obtained. We have studied different noise models as correlated disjoint noise and substitutive noise, which has been shown mathematically that some of those nonlinear correlations are optimum for object location in the presence of such a noise.

In Section 2 we revised the performance of the phase-transformed input joint transform correlator. Section 3 deals with the definition of nonlinear correlation using the phase codification of the joint inputs. Optical experimental results are obtained using a time sequential phase joint transform correlator.

2. Performance of a phase-transformed input joint transform correlator

We review the typical expression for a conversion of an amplitude image in a phase image. The technique of using phase-encoded images, originally represented in gray-levels, has been proven as a process that improves, in general, the performance of optical correlators. As we mention in Section 1, the approach has been implemented in Vander Lugt correlators [11,12], and JTCs [16,17]. The phase encoding of the amplitude transmittance distribution $s(x,y)$ can be expressed as

$$ps(x,y) = \exp\{jT[s(x,y)]\}, \tag{1}$$

where

$$T[s(x,y)] = \frac{s(x,y) - s_{\min}}{s_{\max} - s_{\min}}\pi, \tag{2}$$

where $s_{\max}$ and $s_{\min}$ are the highest and lowest values of $s(x,y)$, respectively. The aim of using a π phase modulation range is to maximize the distance between the maximum and the minimum values of $s(x,y)$ in the complex plane.

As applied to JTC, the phase-encoded input can be written as $ps(x + a,y) + \mathrm{pr}(x - a,y)$, where $pr(x,y)$ is the phase codification of the reference object and a is a constant value that indicates the relative displacement between the two objects. The corresponding joint transform power spectrum is given by

$$\begin{aligned}\mathrm{JPS}(u,v) = {} & |PS(u,v)\exp(-j\phi(u)) \\ & + PR(u,v)\exp(j\phi(u))|^2,\end{aligned} \tag{3}$$

where $PS(u,v)$ and $PR(u,v)$ are the Fourier transforms of $ps(x,y)$ and $pr(x,y)$, respectively, and $\phi(u) = 2\pi ua/(\lambda f)$, with the f focal length of the lens and λ the wavelength of the illumination coherent light.

By an inverse transformation of the JPS, the output light field can be shown as

$$\begin{aligned}C_P(x,y) = {} & ps(x,y) * ps(x,y) + pr(x,y) * pr(x,y) \\ & + ps(x,y) * pr(x,y) \otimes \delta(x - 2a,y) \\ & + pr(x,y) * ps(x,y) \otimes \delta(x + 2a,y),\end{aligned} \tag{4}$$

where $*$ and $\otimes$ denote correlation and convolution, respectively.

In [15], it was shown that under certain conditions the cross-correlation peak between the phase distribution of the scene and the phase distribution of the reference is proportional to an arbitrary constant which is related with the size of the reference function. This value is greater than the one obtained in the conventional JTC. Moreover, it was shown that the phase-encoded input JTC is an optimal filtering system in terms of maximum signal-to-noise (SNR) with additive noise. At the same time, the signal-to-clutter ratio [12] (SCR) was higher than that obtained for the conventional JTC. In the following section, we will show that although the discrimination of those systems is improved in comparison with conventional amplitude JTC, it is not as good as that obtained with the nonlinear correlation define below.

3. Nonlinear correlations using phase input codification

Nonlinear correlations based on binary decomposition were previously described in [23,24]. We now briefly review the essentials. A two-dimensional image with discrete gray levels can be decomposed into a sum of elementary images $e_i[r(x,y)]$ and $e_{\mathrm{th}(i)}[r(x,y)]$ defined as

$$e_i[r(x,y)] = \begin{cases} 1, & r(x,y) = i, \\ 0, & r(x,y) \neq i, \end{cases}$$
$$e_{\mathrm{th}(i)}[r(x,y)] = \begin{cases} 1, & r(x,y) \geqslant i, \\ 0, & r(x,y) < i. \end{cases} \tag{5}$$

The sliced orthogonal nonlinear generalized (SONG) decomposition of $r(x,y)$ using the elementary images $e_i[r(x,y)]$ is

$$r(x,y) = \sum_{i=0}^{Q-1} i e_i[r(x,y)], \tag{6}$$

where Q is the number of gray-levels. At the same time, the image can be defined in terms of the well-known threshold decomposition [28] using the elementary images $e_{\mathrm{th}(i)}[r(x,y)]$ as

$$r(x,y) = \sum_{i=0}^{Q-1} e_{\mathrm{th}(i)}[r(x,y)]. \tag{7}$$

The morphological correlation [23] (MC) between an $s(x,y)$ and $r(x,y)$ is defined as

$$\mathrm{MC}(x,y) = \sum_{i=0}^{Q-1} e_{\mathrm{th}(i)}[s(x,y)] * e_{\mathrm{th}(i)}[r(x,y)]. \tag{8}$$

The MC is a nonlinear correlation that minimizes the mean absolute error (MAE) of the detection instead of the more usual mean squared error (MSE). The MC provides better discrimination capability for pattern recognition tasks than linear correlation and can be implemented optically using a time sequential JTC [23].

The SONG correlation (SONGC) is based on a different binary decomposition, shown in Eq. (6). It is defined as

$$\mathrm{SONGC}(x,y) = \sum_{i=0}^{Q-1} e_i[s(x,y)] * e_i[r(x,y)]. \tag{9}$$

Eq. (8) is a particular definition of a general definition of the SONG correlation presented in [24,26]. Note that the SONGC is defined as the sum of multiple linear correlations between different binary slices of the two functions. This correlation has many properties explained in [24]. For instance it measures the number of common pixels between the two functions for any gray level. We have shown that this correlation is optimum in likelihood sense when images are corrupted with substitutive noise [29]. A weak point of this correlation is that a change in illumination changes the gray level distribution and the correlation result, so the limitation of this scheme is the sensitivity to small intensity or gray level changes which are present in real-world images. In order to alleviate this problem, we showed that the pattern recognition performance can be maintained when the objects are slightly degraded by means of a weighted SONG correlation (WSONG) [25,27].

The SONGC can be implemented optically [26] using the same system as for the morphological correlation [23]. The setup is shown in Fig. 1. Each pair of elementary binary joint input slices

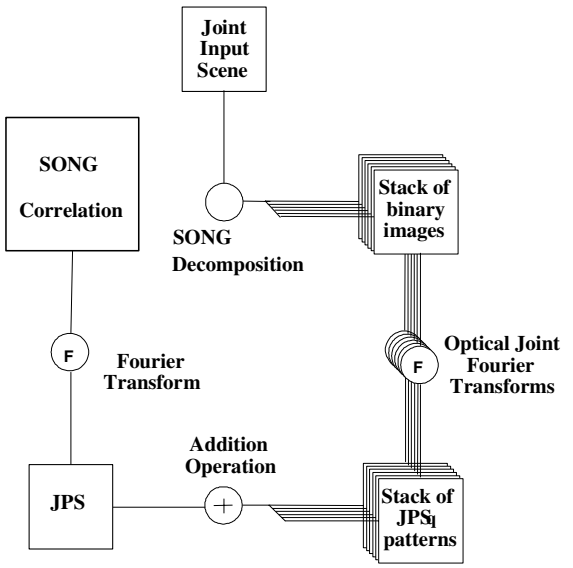

Fig. 1. Block diagram of the optoelectronic nonlinear correlations. The input scene and so, the different binary images are introduced as phase distributions.

(one slice from the reference object and one from the input scene) are placed next to each other in the input plane. For each pair, the joint power spectrum is performed. The summation of the joint power spectrum for all the slices and a second Fourier transformation gives the nonlinear correlation. If the binary representation is defined in terms of the threshold decomposition the MC will be obtained. If the binary representation is the SONG decomposition then the SONGC will be obtained. In all the previous implementations we have used liquid crystal panels working in amplitude modulation. As a novelty in this paper, we will use the same panels working in phase modulation. We will perform a phase-transformed input time sequential JTC to implement the MC and SONGC. These correlation are now defined as

$$\mathrm{PSONGC}(x,y)=\sum_{i=0}^{Q-1} pe_i[s(x,y)] * pe_i[r(x,y)], \tag{10}$$

where

$$\begin{aligned} pe_i[s(x,y)] &= \exp\{\mathrm{j}T[e_i[s(x,y)]]\},\\ pe_i[r(x,y)] &= \exp\{\mathrm{j}T[e_i[r(x,y)]]\}. \end{aligned} \tag{11}$$

So, Eq. (10) represents binary phase distributions with values 0 and π, since only values one and zero are possible for the elementary functions. So, as it was shown in all pattern recognition optical systems, the binarization of the input in JTC is superior to the classical JTC, providing significantly higher peak intensity, a larger peak-to-sidelobe ratio, narrower correlation width and better cross-correlation sensitivity. Moreover, the implementation of PSONGC and PMC (defined as Eq. (9) but changing the subscripts i by th(i)) will have better light efficiency than the linear correlation with phase only gray-scale images (see Eq. (4)) because nonlinear correlations are defined in terms of binary phase distributions. Besides the light efficiency, we will obtain better discrimination than linear correlation as we pointed out in previous references.

So taking into account the setup showed in Fig. 1, and using a phase input, the JPS is

$$\begin{aligned} \mathrm{JPS}_{\Sigma}(u,v) &= \sum_{i=1}^{Q-1}\mathrm{JPS}_i\\ &= \sum_{i=1}^{Q-1}|FT\{pe_i(s)\}|^2+\sum_{i=1}^{Q-1}|FT\{pe_i(r)\}|^2\\ &\quad+\sum_{i=1}^{Q-1}FT\{pe_i(s)\}^{*}FT\{pe_i(r)\}\exp[-\mathrm{i}2\phi_i(u)]\\ &\quad+\sum_{i=1}^{Q-1}FT\{pe_i(s)\}FT\{pe_i(r)\}^{*}\exp[\mathrm{i}2\phi_i(u)]. \end{aligned} \tag{12}$$

The Fourier transform of the third term of Eq. (11) yields the PSONGC. In addition, the Fourier transform of the fourth term is the conjugate of the PSONGC.

4. Noise robustness in the phase nonlinear correlations

One of the aims in pattern recognition is to test the versatility of those operations in images corrupted with different noise sources. We have studied the noise robustness of the PSONGC and the PMC using two noise models: the substitutive noise and the nonoverlapping background noise like disjoint correlated noise. We carried out some computer experiments to determine the stability of various correlation methods in the presence of such noises. We will compare the PSONGC, PMC and the phase linear correlation (see for instance [15,16]).

The substitutive noise is viewed as an impulsive noise or outliers from a statistical point of view. The noise will destroy part of an image, whereas other parts remain unaffected. So an optimum detection solution may be to find a technique for which only this unaffected part will be considered. This is indeed what a specific definition of the SONGC [29] does, because it counts the number of pixels of an image that remain unaffected by the noise. In [29] we demonstrate that SONGC is optimum using maximum likelihood criteria. Now we are introducing a phase codification of the input, so we expect that the PSONGC will have also good performance for recognition in the presence of substitutive noise. Fig. 2 shows the input image used for the compu-

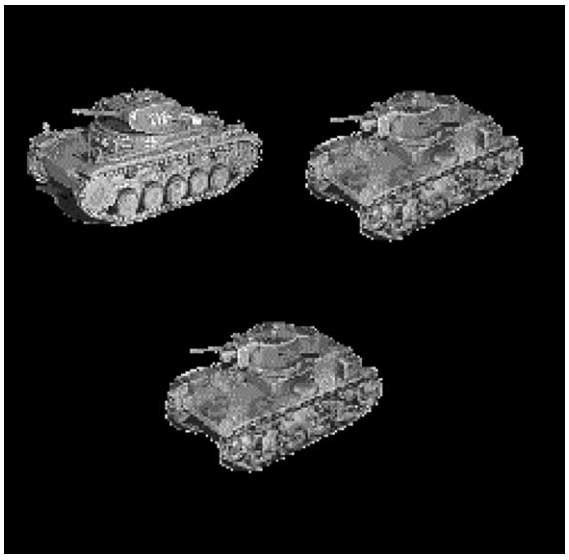

Fig. 2. Input scene containing reference objects (two) and a false object.

ter simulations. This figure contains two different objects. The reference object is the tank placed in the lower part. In order to compare the correlations we have defined the discrimination capability (DC) as

$$\mathrm{DC} = 1 - \frac{\mathrm{CrossCorr}}{\mathrm{AutoCorr}}, \tag{13}$$

where AutoCorr stands for the maximum value of the autocorrelation of the reference, and CrossCorr stands for the maximum value of the cross-correlation between the two objects. A high value of DC means that the value of the cross-correlation is low compared to the auto-correlation, which means that good discrimination and good noise robustness are achieved. On the other hand, a low value of the ratio means that the energy of the cross-correlation has almost the same value as that of the auto-correlation. Fig. 3 is the performance of the DC for the PSONGC, PMC and the phase linear correlation. Note that the DC for the PSONGC is almost constant for the different percentage of number of pixels corrupted. Even for a highly number of pixels corrupted the PSONGC is still able to detect the targets. In Fig. 4 we show an input scene for a 95% of the total amount of pixels corrupted. At the same time,

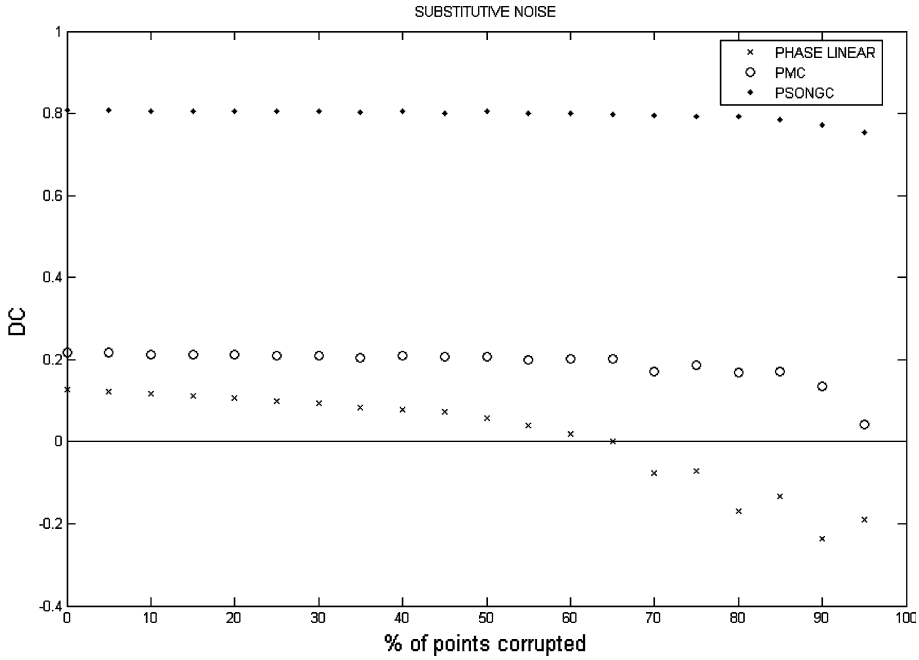

Fig. 3. Performance of the DC for the PSONGC (solid points), the PMC (empty points) and linear correlation with phase-input (cross-lines) when the number of pixel corrupted is varied.

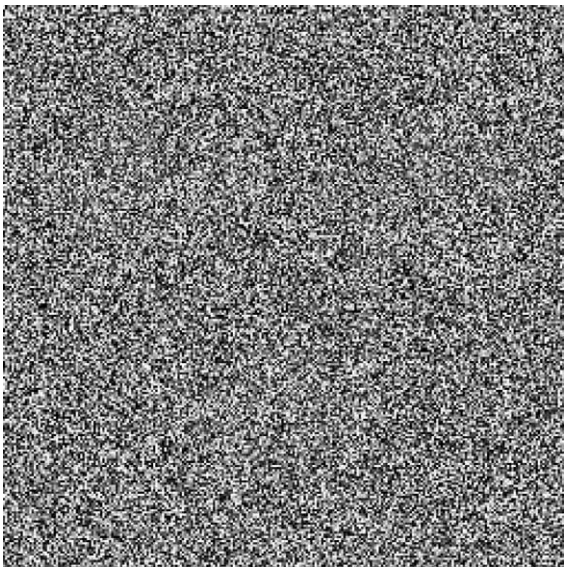

Fig. 4. Input scene shown in Fig. 2, with 95% of the pixels corrupted.

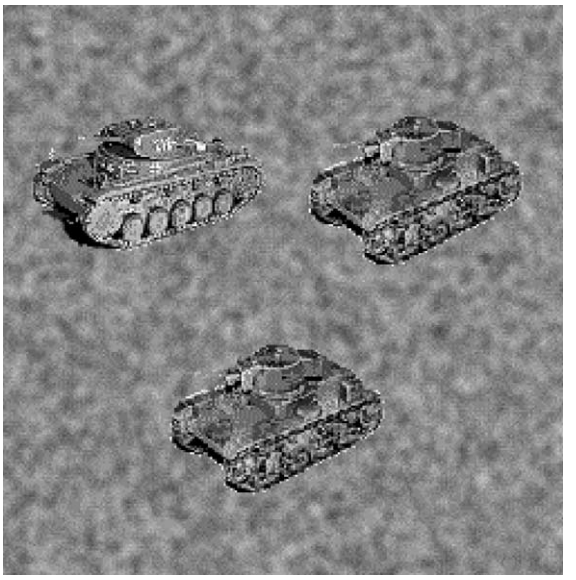

Fig. 6. Input scene with nonoverlapping background noise.

in Fig. 5(a) we show the PSONGC output. In order to compare with the other correlations, in Figs. 5(b) and (c) we show the PMC and the phase linear correlation. Neither the linear nor the morphological is able to detect the target, whereas for the PSONGC the detection is almost perfect.

Regarding the nonoverlapping background noise, in Fig. 6 we show an input image degraded by correlated Gaussian disjoint noise. The mean is a measure of the energy of the pattern where a great value represents a brighter background. As we mention in Section 1, Pagé and Goudail [20] already showed that if the object to be detected is perturbed by nonoverlapping noise, phase encoding can improve the correlation performance compared to amplitude encoding. In Fig. 7 we show the performance of the SCR ratio used also to describe the pattern discriminability. It is defined as

$$\mathrm{SCR} = \frac{\mathrm{AutoCorr}}{\mathrm{CrossCorr}}. \tag{14}$$

The numerator is the autocorrelation peak intensity and the denominator is the maximum cross-correlation peak intensity. In other words, the higher the SCR the higher the pattern discrimina-

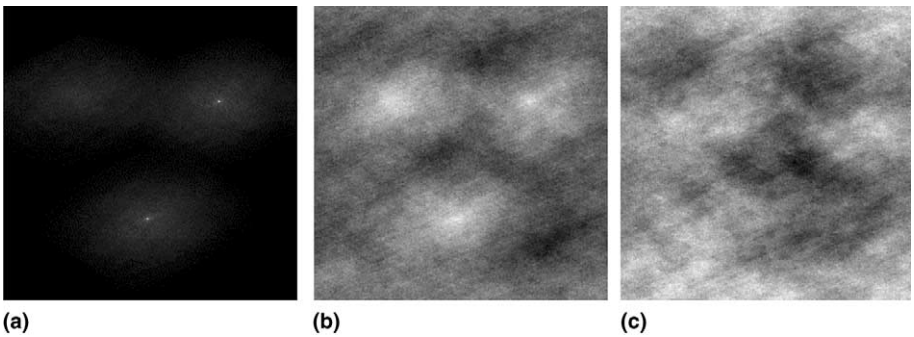

Fig. 5. (a) Correlation plane for the PSONGC, (b) the same for the PMC and (c) the same for the linear correlation with phase-input.

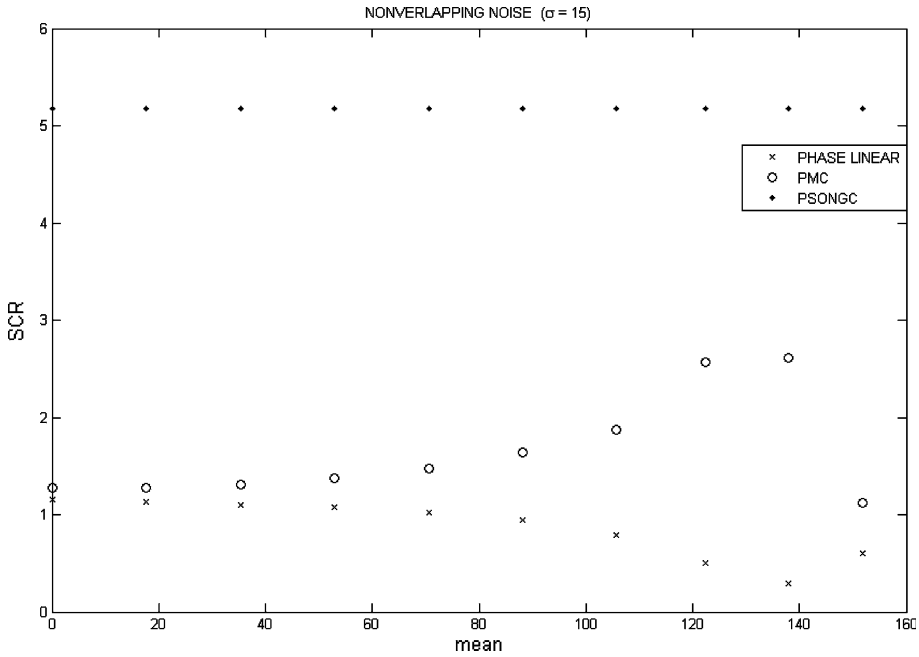

Fig. 7. Performance of the SCR for the PSONGC (solid points), the PMC (empty points) and linear correlation with phase-input (cross-lines) when the mean of the correlated Gaussian noise background is varied.

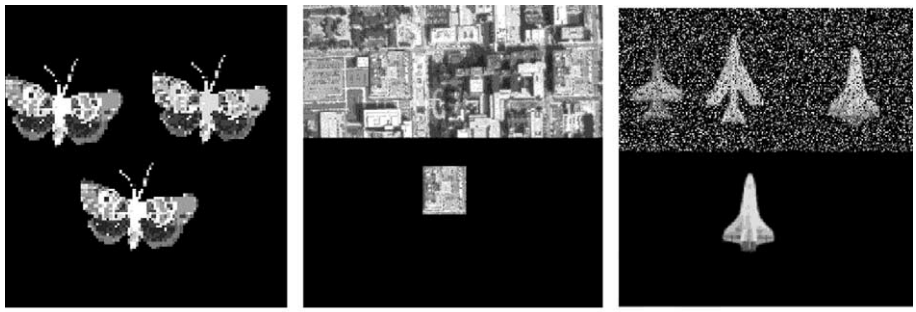

Fig. 8. (a) Joint input scene containing the input scene (top) and the reference object (bottom), (b) joint input scene containing the input scene (top) with the cluttered image and the reference object (bottom), and (c) joint input scene containing the input scene (top) with some amount of substitutive noise, the reference object is placed on the bottom.

bility it would be. We have used this SCR parameter in order to compare with previous references [15,16]. Note that the value of SCR for the PSONGC is almost constant as the noise increases. This stability of the SONGC was already showed in [26]. On the contrary, the performance of linear or morphological is strongly affected by such a noise.

5. Optical experimental results

In previous section, we showed that the PSONGC has excellent performance against substitutive and nonoverlapping background noise. In this section, we have implemented those correlations using a simple joint transform correlation with a SLM working in phase modulation. The

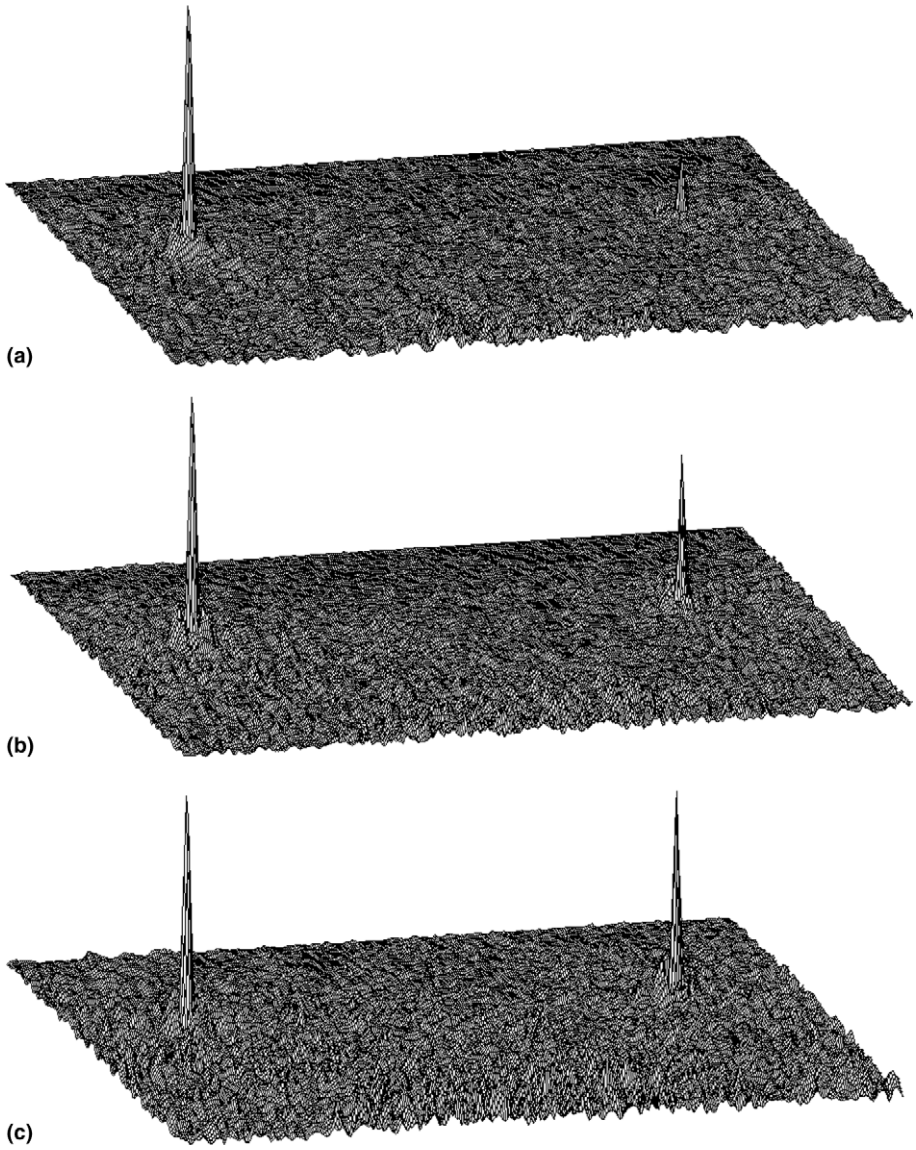

Fig. 9. Experimental output plane containing the optical correlations for the scene shown in Fig. 8(a), where the 3D plots cover an area around the correlation peaks: (a) PSONGC, (b) PMC and (c) phase linear correlation.

SLM that we use for the optical experiments is a XGA LCTV from CRL Smetic Technology. We have calibrated the panel to work as almost phase-only modulator. We have worked with a blue laser ($\lambda = 473$ nm) which provides more than 2π phase modulation range. Binary images are selected with gray levels that correspond to phases 0 and π when addressed to the display. The corresponding joint power spectrums are captured by a CCD camera and then the second Fourier transformation where done digitally.

We have considered three kinds of images for the optical implementation, shown in Figs. 8(a)–(c). The images have eight gray levels. We study the discrimination capability of the PSONGC when the object to be detected is found in the

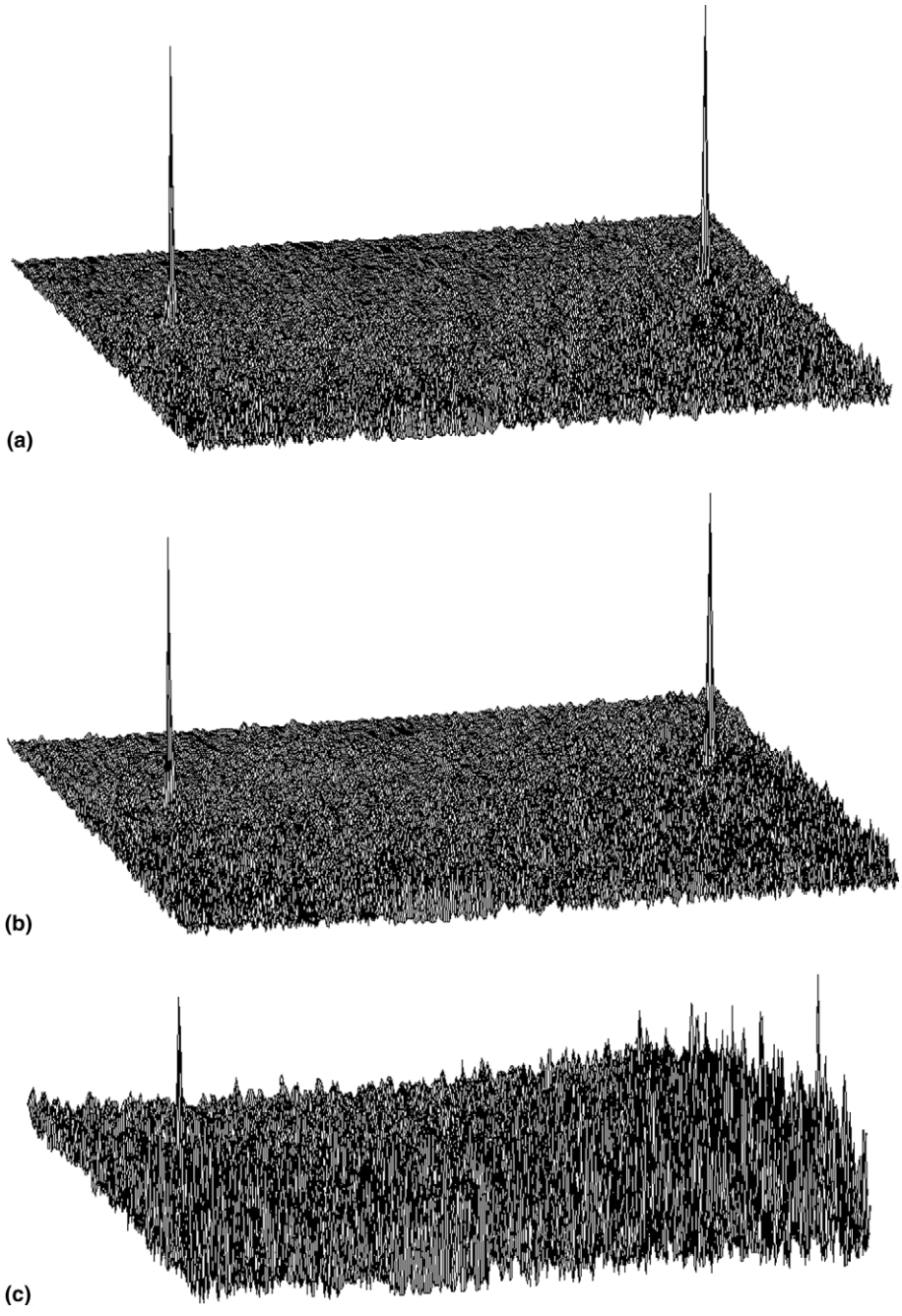

Fig. 10. Experimental output plane containing the optical correlations for the scene shown in Fig. 8(b), where the 3D plots cover an area around the correlation peaks: (a) PSONGC, (b) PMC and (c) phase linear correlation.

presence of other objects and of disjoint noise. Fig. 8(a) contains two butterflies in a dark background. Note that the two butterflies have identical shape but slightly different gray level information. This input image serves to test the discrimination capability for very alike objects in a noise free-case.

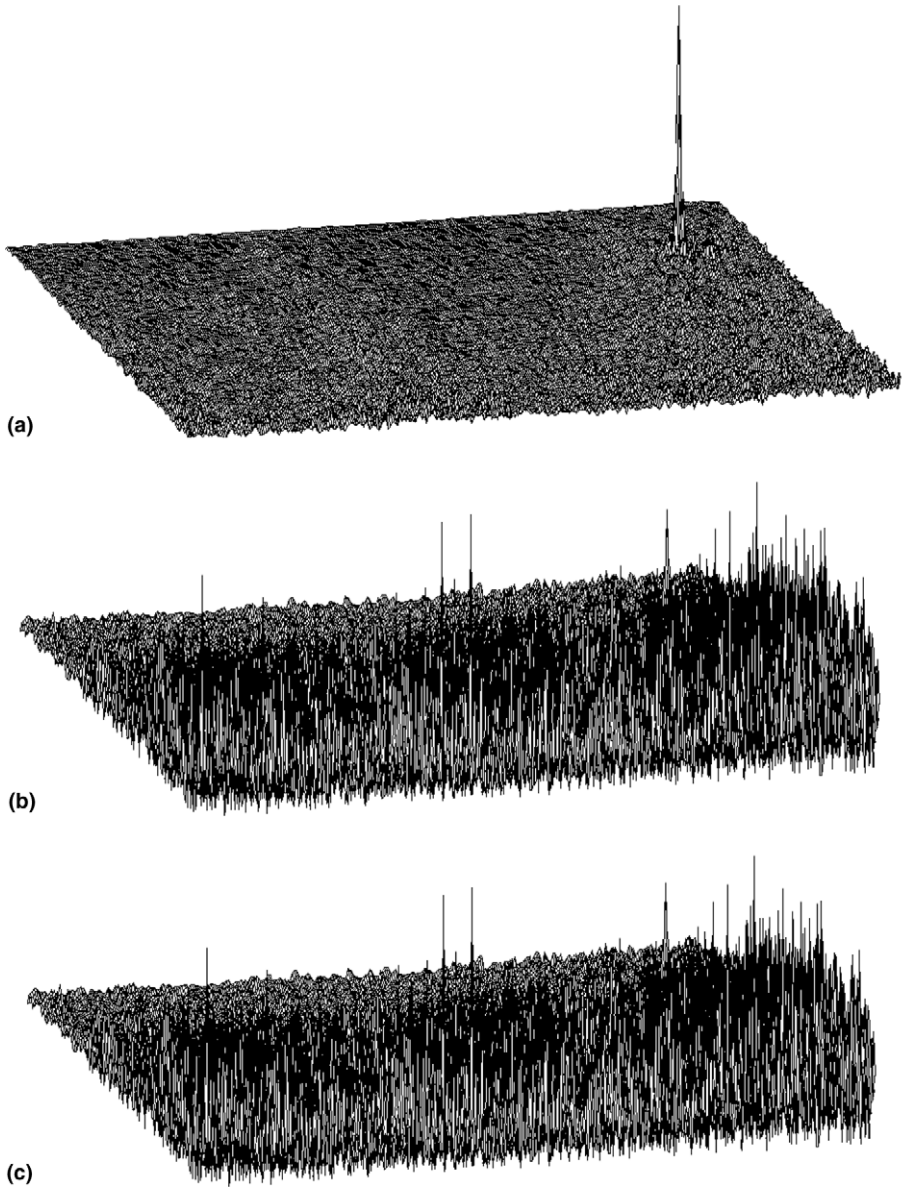

Fig. 11. Experimental output plane containing the optical correlations for the scene shown in Fig. 8(c), where the 3D plots cover an area around the correlation peaks: (a) PSONGC, (b) PMC and (c) phase linear correlation.

Fig. 9(a) shows the result for the PSONGC, Fig. 9(b) shows the result for the PMC and Fig. 9(c) for the linear correlation. Note that we have plotted the optical results only for the region of interest of the correlation. The PMC and the linear phase correlation detect the two butterflies whereas the PSONGC detects the correct, demonstrating its higher discrimination capability.

Another detection case of interest are where the target is in the presence of a highly correlated background, such as building. A city image is shown in Fig. 8(b) where there are two identical

building to be found in a specific place. The PSONGC for Fig. 8(b) is shown in Fig. 10(a) and PMC in Fig. 10(b). The buildings are perfectly isolated from the background. The linear correlation is plotted in Fig. 10(c). Note that the previous correlation fails in the detection.

As a final optical implementation case we have studied the presence of substitutive noise. Fig. 8(c) contains several airplanes where the target is placed at the left part. Fig. 11(a) shows PSONGC when Fig. 8(c) is introduced in the phase JTC. Note that this correlation allows correct detection for the correct target. On the contrary, the PMC (Fig. 11(b)) and the phase linear (Fig. 11(c)) correlations fail again in the detection.

6. Conclusion

We have investigated the performance of nonlinear correlations when the input is phase encoded. The nonlinear correlations are the morphological and the SONG correlations, respectively. We have compared the correlation outputs with the common linear correlation. Although the results for linear correlation with phase-transformed input JTC give better results in pattern discriminability, detection efficiency and noise robustness than common amplitude input JTC, the use of binary decompositions of the input still improves the pattern recognition performance. Moreover, we would like to emphasize that for strong amounts of substitutive noise, the PSONGC is an excellent alternative for pattern recognition where common methods fail.

Acknowledgments

This research was supported by FEDER funds, the spanish Ministerio de Educación y Ciencia, project BFM2001-3004, and la Agencia Valenciana de Ciencia y Tecnologia (AVCT), project GRUPOS03/117.

References

[1] C.S Weaver, J.W. Goodman, Appl. Opt. 5 (1966) 1248.
[2] J.E. Rau, J. Opt. Soc. Am. 56 (1966) 1490.
[3] F.T.S. Yu, X.J. Lu, Opt. Commun. 52 (1984) 10.
[4] B. Javidi, Appl. Opt. 28 (1989) 2358.
[5] B. Javidi, J. Wang, Q. Tang, Appl. Opt. 30 (1991) 4234.
[6] J.L. Horner, Appl. Opt. 21 (1982) 4511.
[7] D. Psaltis, E.G. Paek, S.S. Wenkatesh, Opt. Eng. 23 (1984) 668.
[8] F.M. Dickey, L.A. Romero, Opt. Lett. 14 (1989) 4.
[9] Ph. Réfrégier, Opt. Lett. 16 (1991) 829.
[10] J.L. Horner, P.D. Gianino, Appl. Opt. 26 (1987) 2484.
[11] S. Maze, Ph. Réfrégier, Appl. Opt. 33 (1994) 6788.
[12] R.R. Kallman, D.H. Goldstein, Opt. Eng. 33 (1994) 1806.
[13] F.T.J. Johnson, T.H. Barnes, T. Eiju, T.G. Haskell, K. Matsuda, Opt. Eng. 30 (1991) 1947.
[14] F.T.S. Yu, F. Cheng, T. Nagata, D.A. Gregory, Appl. Opt. 28 (1989) 2988.
[15] G. Lu, Z. Zhang, F.T.S. Yu, Opt. Lett. 20 (1995) 1307.
[16] G. Lu, F.T.S. Yu, Appl. Opt. 35 (1996) 304.
[17] P.S. Erbach, D.A. Gregory, J.B. Hammock, Appl. Opt. 35 (1996) 3091.
[18] S. Ledesma, C. Iemmi, J. Campos, M.J. Yzuel, Opt. Commun. 151 (1998) 101.
[19] C. Iemmi, C. La Mela, Opt. Commun. 209 (2002) 255.
[20] V. Pagé, F. Goudail, Opt. Commun. 175 (2000) 57.
[21] T. Nomura, Appl. Opt. 37 (1998) 3651.
[22] G. Lu, Z. Zhang, S. Wu, F.T.S. Yu, Appl. Opt. 36 (1997) 470.
[23] P. Garcia-Martinez, D. Mas, J. Garcia, C. Ferreira, Appl. Opt. 37 (1998) 2112.
[24] P. Garcia-Martinez, H.H. Arsenault, Opt. Commun. 172 (1999) 181.
[25] M. Tejera, P. Garcia-Martinez, C. Ferreira, D. Lefebvre, H.H. Arsenault, Opt. Commun. 201 (2002) 29.
[26] P. Garcia-Martinez, H.H. Arsenault, S. Roy, Opt. Commun. 173 (2000) 185.
[27] P. Garcia-Martinez, M. Tejera, C. Ferreira, D. Lefebvre, H.H. Arsenault, Appl. Opt. 41 (2002) 6867.
[28] J.P. Fitch, E.J. Coyle, N.C. Gallaguer Jr., IEEE Trans. Acoust. Speech Signal Process. ASSP-32 (1984) 1183.
[29] P. Garcia-Martinez, Ph. Réfrégier, H.H. Arsenault, C. Ferreira, Appl. Opt. 40 (2001) 3855.